Depth Profile of Uncompensated Spins in an Exchange Bias System

S. Roy,[1] M. R. Fitzsimmons,[2] S. Park,[2] M. Dorn,[1] O. Petracic,[1,3] Igor V. Roshchin,[1] Zhi-Pan Li,[1] X. Batlle,[1,4] R. Morales,[1,5] A. Misra,[2] X. Zhang,[2] K. Chesnel,[6] J. B. Kortright,[6] S. K. Sinha,[1,2] and Ivan K. Schuller[1]

[1]*Department of Physics, University of California at San Diego, La Jolla, California 92093, USA*
[2]*Los Alamos National Laboratory, Los Alamos, New Mexico 87545, USA*
[3]*Angewandte Physik, Universität Duisburg-Essen, 47048 Duisburg, Germany*
[4]*Departament de Fisica Fonamental, Universitat de Barcelona, 08028 Barcelona, Catalonia, Spain*
[5]*Departamento de Fisica, Universidad de Oviedo, c/ Calvo Sotel s/n, Oviedo 33007, Spain*
[6]*Lawrence Berkeley National Laboratory, Berkeley, California 94720, USA*

(Received 8 March 2005; published 21 July 2005)

We have used the unique spatial sensitivity of polarized neutron and soft x-ray beams in reflection geometry to measure the depth dependence of magnetization across the interface between a ferromagnet and an antiferromagnet. The net uncompensated magnetization near the interface responds to applied field, while uncompensated spins in the antiferromagnet bulk are pinned, thus providing a means to establish exchange bias.

DOI: 10.1103/PhysRevLett.95.047201 PACS numbers: 75.70.Ak, 61.10.−i, 61.12.−q, 75.70.Cn

Development of magnetic devices, such as spin valves in magnetic recording heads, involves understanding the influence of physical confinement of materials (at the nanometer length scale) on magnetic phenomena [1]. An example is exchange bias [2–6], which is the shift of the ferromagnetic hysteresis loop along the field axis observed in ferromagnet-antiferromagnet (F-AF) systems. The shift is a consequence of exchange coupling across the F-AF interface.

The dependence of exchange bias [2,3] on environmental variables such as field [7–9], temperature [10], and strain [11] is commonly attributed to changes of the domain state [12] in the AF film bulk or at the F-AF interface [13]. Indeed, a neutron scattering study of exchange biased $Co/LaFeO_3$ [14] and an x-ray magnetic circular dichroism study of exchange biased $Co/Ir_{0.8}Mn_{0.2}$ [15] observed correlations between exchange bias and pinned magnetization in the AF. In order to understand exchange bias in terms of spin structure, there is a compelling need to determine the distribution of uncompensated magnetization at the F-AF interface and in the AF bulk and the response of uncompensated magnetization to field.

We have used polarized neutron and soft x-ray beams in reflection geometry to measure the depth profile of magnetization across the F-AF interface and inside the AF film with unprecedented sensitivity. Measurement with neutron beams provides the variation of the *vector* magnetization (projected onto the sample plane) in absolute units, and measurement with circularly polarized x-ray beams tuned to the L edges of the magnetic atoms provides the variation of the element specific magnetization projected onto the incident beam axis [16–18].

Exchange bias samples were prepared by sequential electron beam evaporation of FeF_2, Co, and Al at a deposition rate of 0.05 nm/s onto (110) oriented single crystal MgF_2 polished substrates measuring 10 mm by 10 mm. The deposition temperatures were 300 °C for the FeF_2 layer and 150 °C for the Co and Al layers. The chemical structure of the sample was determined from nonresonant x-ray reflectometry. The thickness of the Co (FeF_2) layer was 4.1 ± 0.1 nm (36.6 ± 0.1 nm), and the structural roughness of the Co/FeF_2 (FeF_2/MgF_2) interface was 0.5 ± 0.1 nm (0.4 ± 0.1 nm). A comparison of the off-specular x-ray reflectivity to the specular x-ray reflectivity [19] indicates that the roughnesses of the two interfaces were uncorrelated.

In-plane glancing angle x-ray diffraction and transmission electron microscopy confirmed that the AF layer was an untwinned single crystal film with $[1\bar{1}0]$ $FeF_2 \parallel [1\bar{1}0]$ MgF_2 and surface normal along [110] FeF_2 [20]. The $\sim 1.8°$ widths of in-plane Bragg reflections from the FeF_2 single crystal were 4 times broader than the reflections from the MgF_2 substrate. The dislocation density [21] at the FeF_2/MgF_2 interface corresponds to an average spacing between dislocations of ~55 nm, rather than 21 nm anticipated for this interface were all the misfit strain relieved [22]. Therefore, only a fraction of the total misfit strain is relieved in the FeF_2 film. Defects and strain can produce uncompensated magnetization in FeF_2 via piezomagnetism [11].

The resonant soft x-ray scattering experiment was performed using a circularly polarized incident x-ray beam (Fig. 1). The sample was cooled to 20 K in a field of $H_{FC} = 796$ kA/m applied along [001] FeF_2 (to establish positive bias). The sample and detector were rotated about $[\bar{1}10]$ FeF_2. The intensity of the specularly reflected radiation was recorded as a function of incident beam polarization, applied field H, and wave vector transfer Q ($= k_f - k_i$, Fig. 1). The incident x-ray wavelength was tuned to either the Co-L_3 or Fe-L_3 edge with the signs of the charge and magnetic scattering factors the same. In the first measurement, the angles of incidence and reflection were fixed at 3° relative to the sample surface, and the reflected intensity was recorded for left and right circularly polarized light,

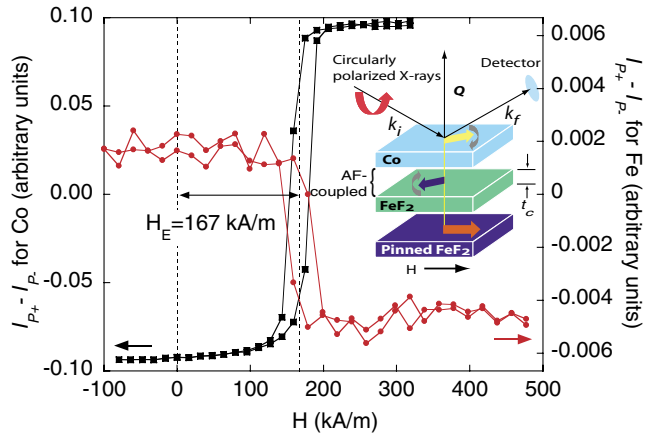

FIG. 1 (color). Hysteresis loops at $Q = 0.49$ and 0.38 nm^{-1} for Co (■) and Fe (red ●), respectively. Inset: representations of the x-ray experiment and sample.

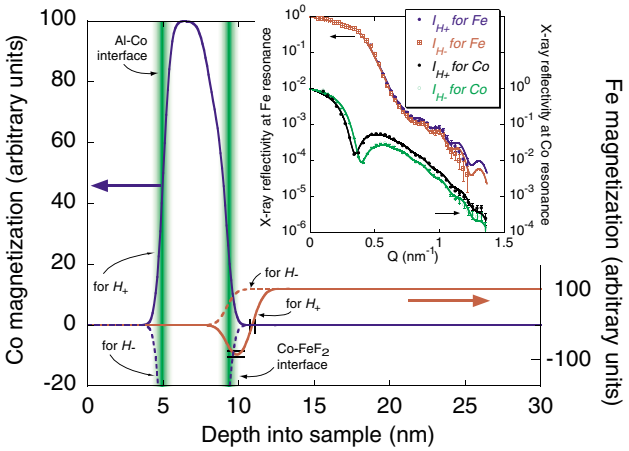

FIG. 2 (color). Spin density depth profiles for Co (blue) and Fe (red) spins obtained from the specular x-ray reflectivities (inset) at $H_{\pm} = \pm 796$ kA/m.

I_{P+} and I_{P-} (polarization = ±90%) as a function of H. Magnetization loops (Fig. 1) corresponding to Co (■) or Fe (red ●) spins [23] exhibit hysteresis indicating that some Co and Fe spins are unpinned. Both loops are shifted by the bias field $H_E = +167 \pm 4$ kA/m. Since the coercivity and bias obtained from either loop are the same, the Co and Fe spins are likely coupled. Along the magnetization axis, the curves are inverted, suggesting an antiparallel arrangement of Co and Fe spins [24].

We performed a second soft x-ray experiment that involved measuring the reflected intensity of one incident beam polarization as a function of Q, and $H = \pm 796$ kA/m. This protocol is sensitive to changes in the specular reflectivity due to the reversal of unpinned spins. From the variation of I_{H+} and I_{H-} with Q (Fig. 2, inset)—the subscript refers to H parallel (+796 kA/m) or antiparallel (−796 kA/m) to $H_{FC} \parallel [001]$ FeF_2—the depth profiles of the Co and Fe spins can be obtained for each field direction. In modeling these profiles, the Co magnetization was considered to be unpinned, but the possibility for having both unpinned Fe spins and Fe spins pinned along H_{FC} was retained. Using a generalization of the distorted wave Born approximation including resonant scattering of soft x-rays [16–18], the reflectivities for the two directions of H were calculated from the spin density profiles (Fig. 2) to obtain the solid curves (inset, Fig. 2) that minimized χ^2 [25]. The spin profiles represent the projections of the net magnetization of Co or Fe onto the incident beam axis—the latter is nearly parallel (or antiparallel) to H [26]. We see a change of the Fe spin magnetization from negative to positive over a distance of ~2 nm *below* the Co/FeF_2 interface for H_+ (red solid curve, Fig. 2)—indicating that the Fe and Co spins are antiparallel across the interface for this field. The distance of 2 nm is much larger than that corresponding to interdiffusion or chemical roughness across the Co/FeF_2 interface; therefore, variation of Co and Fe spin density might be attributed to magnetic domains at the interface, or to the rotation of magnetization away from the field axis. For H_-, the Co spin density profile is negative (blue dashed curve, Fig. 2) and the Fe spin density profile is positive (red dashed curve, Fig. 2)—again indicating that the Fe and Co spins are antiparallel across the interface.

We undertook a polarized neutron reflectometry [27,28] study with polarization analysis to determine whether the spatial variation of the net magnetization vector [29] in the Co and FeF_2 layers could be attributed to a domain wall parallel to the Co/FeF_2 interface, and to obtain the depth profile of the pinned magnetization. After cooling the sample to 10 K in a 438 kA/m field along [001] FeF_2 (to establish bias), we rotated the sample about its surface normal in this field, so that H was parallel to $[\bar{1}10]$ FeF_2 (Fig. 3, inset). This protocol enables separation of the magnetization vector depth profile into unpinned and/or pinned components. The polarized neutron reflectivity of the sample is shown in Fig. 3, after removal of instrumental background and correction for polarization efficiencies [19]. The large difference between the two nonspin-flip (NSF) reflectivities (R^{++} and R^{--}) is related to the component $M_{\parallel}$ of the net magnetization vector that follows H and lies in the sample plane. The spin-flip (SF) reflectivity R^{SF} (the average of the intensities of the neutron beam whose polarization is flipped from spin-up to down, and vice versa) [Fig. 3 (green symbols)] is related to the component $M_{\perp}$ of the net magnetization vector that is perpendicular to H and lies in the sample plane. From R^{NSF} and R^{SF}, the depth profile of the net magnetization vector projected onto the sample plane is obtained quantitatively. Even in the absence of quantitative fitting (discussed later), observation of nonzero SF reflectivity means that the field of 438 kA/m applied parallel to $[\bar{1}10]$ FeF_2 during the neutron measurement was not sufficient to rotate the entire sample magnetization from [001] FeF_2 (the direction of the cooling field) to $[\bar{1}10]$ FeF_2. We regard the portion of the magnetization that does not respond to

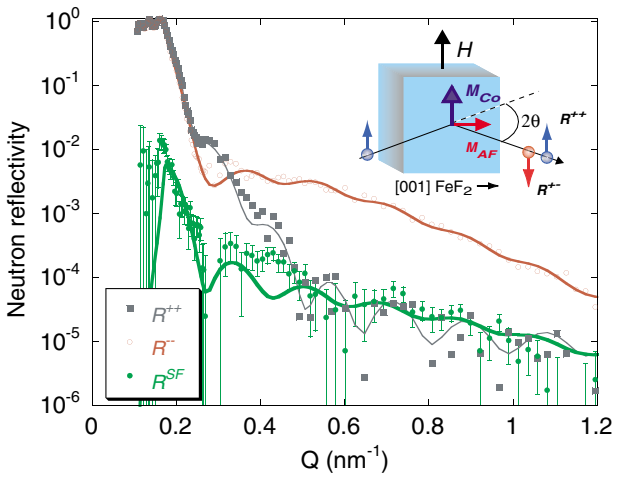

FIG. 3 (color). Polarized neutron reflectivity (symbols) measured with field along $[\bar{1}10]$ FeF_2. The solid curves were calculated from a model whose magnetization depth profile is shown in Fig. 4. Inset: representation of the neutron experiment.

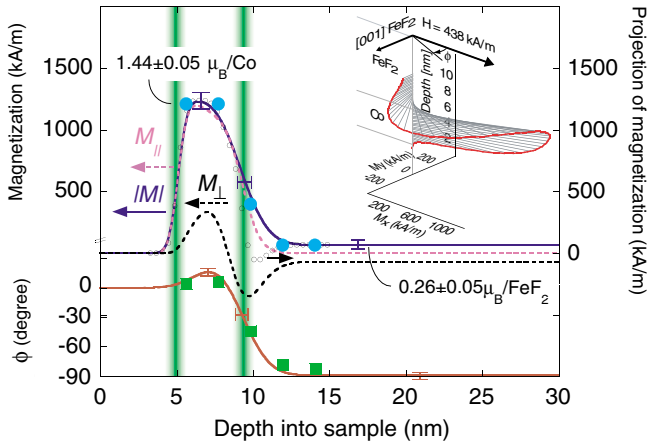

FIG. 4 (color). Depth dependence of the vector magnetization (inset, 3D view), magnitude (blue curve, $|M|$), and angular deviation ϕ (red curve) from the applied field in the sample plane deduced from neutron scattering. Error bars represent deviations of depth profiles with indistinguishable χ^2. The magnetization used in the OOMMF simulation (cyan ●) and the values of ϕ (green ■) obtained from the simulation. The sum of the Fe and Co spin density profiles for $H \parallel [001]$ FeF_2 (obtained from Fig. 2 in arbitrary units using x-ray scattering) is shown in absolute units (○).

the applied field applied as pinned along [001] FeF_2. We note that SF reflectivity was not observed when the field applied during the neutron measurement was parallel to [001] FeF_2. Nor was SF reflectivity observed when the field was applied parallel to $[\bar{1}10]$ FeF_2 *and* the temperature of the sample was 108 K—significantly above the ordering temperature $T_N = 78$ K of FeF_2.

Quantitative information about the locations of unpinned and pinned uncompensated magnetization in the sample was obtained from an analysis of the Q dependence of the neutron reflectivity using the Parratt formalism [30]. The magnetic structure of the model was divided into three regions representing magnetization in the Co layer (with magnitude M_{Co} [31] and direction ϕ_{Co} in the sample plane relative to the applied field), the interface (M_{int}, ϕ_{int}), and the FeF_2 bulk ($M_{\mathrm{FeF_2}}$, $\phi_{\mathrm{FeF_2}}$). The magnetization of one region was connected to the next using an error function each with an adjustable width σ [32]. The magnetic thickness of the interface was adjusted at the expense of the FeF_2 magnetic layer thickness. These eight parameters were optimized to minimize χ^2 which yielded the magnetization depth profile (Fig. 4).

The magnetization in the Co film is mostly parallel to H except near the Co/FeF_2 interface where the magnetization rotates in the positive sense away from the applied field by $\phi_{\mathrm{Co}} = +16°$ (red curve, Fig. 4). The uncompensated magnetization in the FeF_2 rotates in the opposite sense to be $\phi_{\mathrm{int}} = -30°$ near the Co/FeF_2 interface and then parallel to [001] FeF_2 in the AF film bulk ($\phi_{\mathrm{FeF_2}} = -89 \pm 5°$) [33]. The tendency for the Co magnetization and the net uncompensated magnetization in the FeF_2 to rotate in opposition is evident in the change of sign of the component of the magnetization perpendicular to the applied field $M_\perp = M(z)\sin[\phi(z)]$ (dashed black curve, Fig. 4) [34]. The twist of the magnetization across the Co/FeF_2 interface is reminiscent of a domain wall parallel to the interface between soft and hard magnetic materials, as found, for example, in exchange spring magnets [35,36] or as proposed by Kiwi *et al.* [37] to explain exchange bias in Fe/FeF_2 bilayers. The rotation of the uncompensated magnetization close to the Co/FeF_2 interface provides a natural explanation for the experimental observation that an antiferromagnet must exceed a critical thickness, t_c (Fig. 1), before bias can be produced [38].

In a previous study of the influence of crystalline quality of Co/FeF_2 films on exchange bias [39], exchange bias was found to be small for single crystal FeF_2 films grown on FeF_2 bulk single crystals—a recipe that minimizes misfit strain in the thin film lattice—in contrast to the substrate (MgF_2) reported here. The accommodation of misfit strain through the formation of defects may be an important factor affecting the antiferromagnetic domain state and exchange bias. We note that previously large exchange bias in $Co/Co_xO_{(1-x)}$ bilayers was attributed to uncompensated magnetization in the bulk of nonstoichometric CoO [12].

We used the micromagnetic simulation package OOMMF [40] to determine whether the magnetization profile deduced from neutron scattering was consistent with a low energy magnetic configuration for the conditions of our experiment. We treated the interface and uncompensated spins in the FeF_2 layers as if they were slightly ferromagnetic and assigned saturation magnetizations of 1212, 400, and 67 kA/m to the Co, interface, and FeF_2 layers, respectively, to mimic the magnetization profile in Fig. 4 (cyan ●). Values for the exchange stiffness of 30×10^{-12}

and 1.23×10^{-12} J/m were used for Co and FeF_2, respectively, and the average of these values assigned to the interface layer. Values for the uniaxial anisotropy of 4.5×10^5 and 1.76×10^6 J/m^3 were used for Co and FeF_2, respectively. We included two adjustable parameters in the simulation—the interface exchange constant J_{int} across the interface between the Co and interface layers and the anisotropy of the interface K_{int}. Values of $J_{\text{int}} = -1.5 \times 10^{-3}$ to -2.0×10^{-3} J/m^2 and $K_{\text{int}} = 1 \times 10^5$ J/m^3 yield the direction of the vector magnetization in Fig. 4 (green ■), in good agreement with the neutron scattering result, thus confirming that the magnetization depth profile shown in Fig. 4 is a low energy configuration. The micromagnetic simulation was repeated using the same magnetic model but with the field applied along [001] FeF_2 and varied between ± 477 kA/m. With the initial configuration of all three layers aligned in the positive direction, which is equivalent to cooling the sample in a large magnetic field, the simulation yielded a positively shifted hysteresis loop. This confirms that due to large anisotropy, the moments in the bulk FeF_2 remain pinned in the initial direction.

In conclusion, we have performed experiments to measure the depth profiles of the pinned and unpinned magnetization in a Co/FeF_2 system that exhibits $+167$ kA/m exchange bias. We found uncompensated magnetization in the (nominally) antiferromagnetic FeF_2 layer. Within 2 to 3.5 nm of the Co/FeF_2 interface, the uncompensated FeF_2 magnetization is antiparallel to the Co spins and rotates in conjunction with the Co spins. However, at distances greater than $\sim$3.5 nm from the interface, the uncompensated FeF_2 magnetization is pinned, providing a means to establish bias.

The facilities of the Manuel Lujan, Jr. Neutron Scattering Center and the Advanced Light Source are gratefully appreciated. Discussions with M. J. Donahue, D. Lederman, K. Liu, and R. D. McMichael are gratefully acknowledged. This work was supported by the Office of Basic Energy Science, U.S. Department of Energy, BES-DMS, the University of California Campus Laboratory Collaborative program, and Laboratory Directed Research and Development program funds. Financial support from the Alexander-von-Humboldt Foundation (O. P.), Cal(IT)^2 (Z.-P. L.), Spanish MECD (R. M. and X. B.), Fulbright Commission (R. M.), Catalan Dursi (X. B.), and the Swiss National Science Foundation (M. D.) is acknowledged.

[1] M. R. Fitzsimmons *et al.*, J. Magn. Magn. Mater. **271**, 103 (2004).
[2] W. H. Meiklejohn, and C. P. Bean, Phys. Rev. **105**, 904 (1957).
[3] J. Nogués and I. K. Schuller, J. Magn. Magn. Mater. **192**, 203 (1999).
[4] A. E. Berkowitz and K. Takano, J. Magn. Magn. Mater. **200**, 552 (1999).
[5] R. L. Stamps, J. Phys. D: Appl. Phys. **33**, R247 (2000).
[6] M. Kiwi, J. Magn. Magn. Mater. **234**, 584 (2001).
[7] M. R. Fitzsimmons *et al.*, Phys. Rev. Lett. **84**, 3986 (2000).
[8] I. N. Krivorotov *et al.*, Phys. Rev. B **68**, 54430 (2003).
[9] A. Hoffmann, Phys. Rev. Lett. **93**, 097203 (2004).
[10] H. Shi *et al.*, J. Appl. Phys. **93**, 8600 (2003).
[11] Ch. Binek *et al.*, J. Magn. Magn. Mater. **240**, 257 (2002).
[12] P. Miltényi *et al.*, Phys. Rev. Lett. **84**, 4224 (2000).
[13] Hongtao Shi *et al.*, J. Appl. Phys. **93**, 8600 (2003).
[14] A. Hoffmann *et al.*, Phys. Rev. B **66**, 220406 (2002).
[15] H. Ohldag *et al.*, Phys. Rev. Lett. **91**, 017203 (2003).
[16] S. A. Stepanov and S. K. Sinha, Phys. Rev. B **61**, 15302 (2000).
[17] D. R. Lee *et al.*, Phys. Rev. B **68**, 224409 (2003).
[18] R. M. Osgood III *et al.*, J. Magn. Magn. Mater. **198-199**, 698 (1999).
[19] S. Park *et al.*, Phys. Rev. B **70**, 104406 (2004).
[20] The (110) plane of FeF_2 is normally compensated.
[21] D. B. Williams and C. B. Carter, *Transmission Electron Microscopy* (Plenum, New York, 1996), p. 447.
[22] L. B. Freund, MRS Bull. **17**, 52 (1992).
[23] L_3 edges of Co and Fe occur at different x-ray wavelengths, so measurements taken at the same scattering angles have slightly different Q.
[24] In switching the polarization of the x-ray beam, the vertical shift changed magnitude and sign. We conclude the vertical shift is an instrumental artifact. The exchange bias, coercivity, and inversion of the Fe loop with respect to the Co loop were reproducible.
[25] P. R. Bevington and D. K. Robinson, *Data Reduction and Error Analysis for the Physical Sciences* (McGraw Hill, New York, 2003), 3rd ed., p. 67.
[26] We used neutron scattering to establish an absolute scale for the x-ray results.
[27] G. P. Felcher *et al.*, Rev. Sci. Instrum. **58**, 609 (1987).
[28] C. F. Majkrzak, Physica B (Amsterdam) **221**, 342 (1996).
[29] Our study is not sensitive to canting of the sample magnetization out of the sample plane.
[30] L. G. Parratt, Phys. Rev. **95**, 359 (1954).
[31] M_{Co} was obtained from neutron data collected at 108 K.
[32] The magnetic interface widths were 1.5 ± 0.1 nm.
[33] The neutron scattering data are sensitive to the orientation of the FeF_2 magnetization relative to the Co magnetization; in particular, these magnetizations move in opposite directions.
[34] The refinement started with magnetization twisting in the same direction across the Co/FeF_2 interface, yet evolved towards a structure having the Co magnetization rotating in opposition to the FeF_2 magnetization.
[35] O. Hellwig *et al.*, Phys. Rev. B **62**, 11694 (2000).
[36] K. V. O'Donovan *et al.*, Phys. Rev. Lett. **88**, 067201 (2002).
[37] M. Kiwi, J. Mejía-López, R. D. Portugal, and R. Ramírez, Appl. Phys. Lett. **75**, 3995 (1999).
[38] M. S. Lund *et al.*, Phys. Rev. B **66**, 054422 (2002).
[39] M. R. Fitzsimmons *et al.*, Phys. Rev. B, **65**, 134436 (2002).
[40] M. J. Donahue and D. G. Porter, *OOMMF User's Guide Version 1.0," NISTIR 6376* (National Institute of Standards and Technology, Gaithersburg, MD, 1999).